

Resonant Tunneling Mediated by Resonant Emission of Intersubband Plasmons

K. Kempa

Department of Physics, Boston College, Chestnut Hill, Massachusetts 02467-3811

E. Gornik, K. Unterrainer, M. Kast, and G. Strasser

Institute for Solid State Electronics and Microstructure Center, Technische Universitat Wien, A-1040 Wien, Austria

(Received 14 November 2000)

We study tunneling through resonant tunneling diodes (RTD) with very long emitter drift regions (up to $2 \mu\text{m}$). In such diodes, charge accumulation occurs near the double barrier on the emitter side, in a self-induced potential pocket. This leads to a substantial enhancement of the wave function overlap between states of the pocket and the RTD, and, consequently, to increased off-resonant current mediated by various scattering processes. For RTD with the longest drift region ($2 \mu\text{m}$), an additional strong current peak is observed between the first and the second resonant peaks. We attribute this pronounced feature to the intersubband transitions mediated by resonant emission of intersubband plasmons.

DOI: 10.1103/PhysRevLett.86.2850

PACS numbers: 72.10.-d, 71.45.-d, 73.20.Mf

Resonant tunneling diodes (RTD) have been studied thoroughly [1] both theoretically and experimentally since their conception in 1974 by Tsu and Esaki [2]. Many direct and indirect applications of RTD's have been investigated [3]. However, there remain still unresolved problems especially in the off-resonant domain, where the current is mediated by various intersubband scattering processes. It has been demonstrated that the transport through RTD can be mediated by the longitudinal-optic (LO) phonons [4], photons [5], two-dimensional (2D) plasmons [6], electron-electron scattering [7], and elastic electron scattering with defects (impurities and interface imperfections) [8]. In this Letter, we report the first observation of the off-resonant tunneling mediated by the resonant electron-intersubband plasmon scattering.

The GaAs-GaAlAs modulation doped structures used in this study consist of the following: 4000 \AA of GaAs top contact (emitter) layer Si doped to $1.5 \times 10^{18} \text{ cm}^{-3}$; an undoped drift region layer of thickness D ; RTD with 80 \AA barrier (GaAlAs, $x = 0.32$), 195 \AA GaAs quantum well, and 60 \AA barrier (GaAlAs, $x = 0.32$); 15 \AA GaAs spacer; 1000 \AA GaAs layer Si doped to $1 \times 10^{16} \text{ cm}^{-3}$; and 4000 \AA GaAs contact (collector) layer Si doped to $1.5 \times 10^{18} \text{ cm}^{-3}$. Three samples with $D = 0.1 \mu\text{m}$ (sample A), $1 \mu\text{m}$ (sample B), and $2 \mu\text{m}$ (sample C) were grown. The corresponding current-voltage (I - V) characteristics of the three samples for biases, such that the electrons flow into RTD from the extended emitter drift region, are shown in Fig. 1. The curves are very similar, except for the appearance of a strong peak (marked by an arrow) between the first and the second resonant peaks, in sample C. There is also an overall reduction of the width of the resonant peaks for samples B and C, and an increase of the off-resonant current for sample B. In order to understand these experimental results, we have performed a series of various calculations and additional experiments.

A self-consistent calculation [9] of the nonequilibrium steady state of our RTD's shows that, in structures with very long emitter drift regions ($1 \mu\text{m}$ or more), a potential pocket self-induces on the emitter side. This is shown in Fig. 2, which displays the calculated self-consistent Thomas-Fermi nonequilibrium steady state potential for samples A and C. The result for sample B is essentially identical with that for sample C. This calculation requires an assumption of the degree of charge accumulation across an entire structure. In the heavily doped regions, which act as electron reservoirs, one can easily define the Fermi level (we assume $T \approx 0$). We assume that there is no voltage drop across the drift region, i.e., it is in equilibrium with the emitter reservoir. The RTD has a "thinner" barrier (60 \AA) on the collector side, and therefore it might be considered empty for the biases

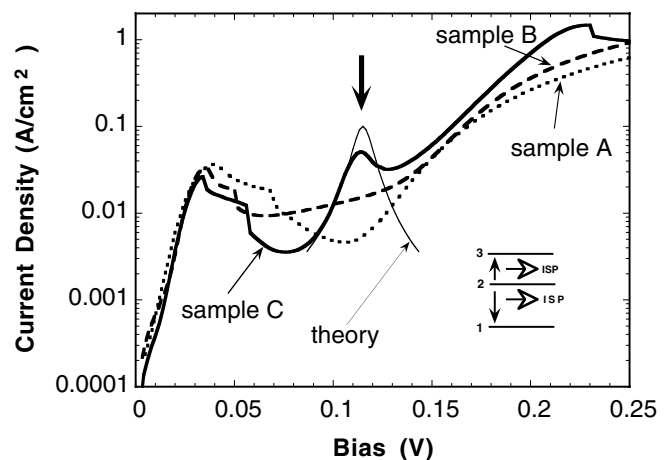


FIG. 1. Current density versus the applied bias for our RTD structures. Inset shows a scheme of intersubband transitions in sample C, which lead to formation of the additional peak indicated by an arrow. The thin solid line represents the theoretical result.

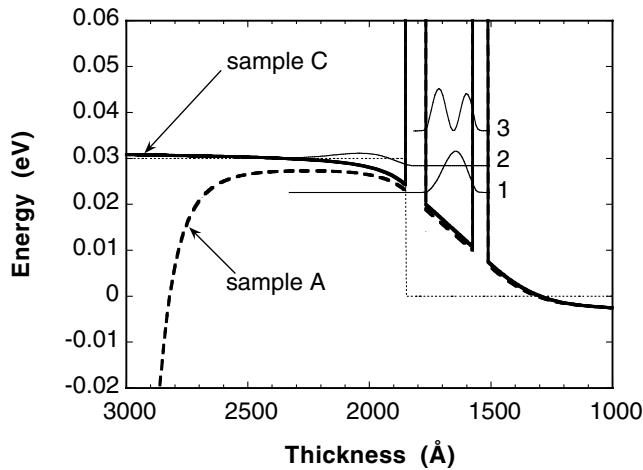


FIG. 2. The conduction band edge for samples *A* and *B* versus distance, in the vicinity of the double barrier for the bias corresponding to the additional peak shown in Fig. 1. Dotted line represents the quasi-Fermi level. The thin solid lines show squares of wave functions of the relevant subbands.

of interest. This allows one to determine the screened potential uniquely in this calculational scheme.

The fact that the tunneling in sample *A* occurs essentially from the emitter reservoir, while for sample *B* (and also *C*) it occurs from the self-induced pocket at the RTD, immediately explains why the first resonant tunneling peak for sample *A* is much broader than that for sample *B* (and *C*). Since the resonant peaks of Fig. 1 essentially “project” the density of states of the occupied states on the emitter side, the broad band of continuum of states in sample *A* shows up as broad resonant peaks in Fig. 1. For samples *B* and *C*, the tunneling occurs for low biases essentially from the single subband of the pocket, which accounts for the “narrowness” of the first resonant peak for these samples.

The overall larger off-resonant current in sample *B*, as compared with sample *A*, can be explained by the much larger electron density in the RTD of sample *B* due to formation of the potential pocket. This is essentially similar to the alpha decay process [10], and can be easily understood classically. Reducing L (the pocket size) increases the frequency of “strikes” by trapped electrons against the barrier of the RTD. While, in sample *A*, $L = D = 0.1 \mu\text{m}$, in samples *B* and *C*, $L \sim 200 \text{ \AA}$. The resulting much larger electron density inside RTD allows for the electron-defect [8], or the electron-electron (Auger) [11] scatterings to mediate the intersubband electron transport. In these elastic processes, the dominant transitions involve an electron, scattering from the initial (emitter) subband 2, into the lower subband 1 (the lowest subband of RTD) “horizontally” on the energy momentum diagram, i.e., with no energy, but large momentum exchanged. The phase space for such transitions is not sensitive to the relative positions of the two subbands, and therefore there is no reason for an enhancement of the scattering rate at a particular bias.

This results in an enhancement of the off-resonant current in a wide range of biases.

In the sample with even larger drift region (sample *C*, $L = 2 \mu\text{m}$), an additional peak appears at the intermediate bias between the first and the second resonant peaks (see Fig. 1). The peak cannot be due to electron-defect, or electron-electron Auger scattering, which are bias insensitive. Since the relevant intersubband separations are less than 35 meV, the electron-LO phonon scattering is suppressed, and also cannot explain the peak.

To understand this feature, we must consider the electron-electron scattering process. The electron-electron scattering rate γ_{scat} is given directly by the imaginary part of the electron self-energy [12]. It can be shown that, in the random phase approximation, γ_{scat} has the convenient form of the golden rule, with the screened interaction replacing the bare Coulomb interaction [13]. This form explicitly shows that singularities of the screened Coulomb interaction (collective modes) will strongly contribute to the scattering. Electron-electron scattering mediated by emission of 2D plasmons of the electron gas trapped in RTD was indeed observed in Ref. [6]. In our RTD, an intersubband plasmon (ISP) can be excited, which can lead to strong enhancement of the electron-electron scattering.

The properties of ISP are illustrated in Ref. [12], through calculation of the screened Coulomb interaction in a model system consisting of two subbands, with the subband separation Δ . Figure 3 (taken from Ref. [12]) shows the absorption spectrum (essentially imaginary part of the screened interaction) vs the normalized frequency ω/Δ , calculated for this model. The solid line is for the in-plane wave vector $q = 0.3k_F$, dotted for $q = 0.6k_F$, and dashed for $q = 1.2k_F$, where k_F is the Fermi wave

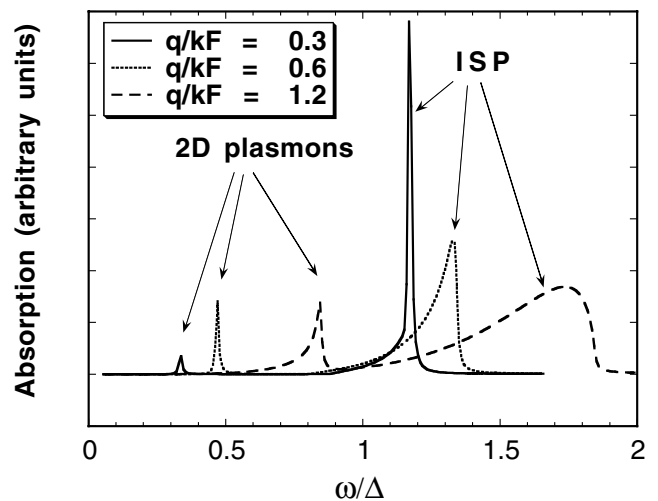


FIG. 3. The absorption spectrum versus the normalized frequency, for a two subband model and for various values of the in-plane wave vector q .

vector. The low frequency feature on each curve (for $\omega/\Delta < 1$) is the 2D plasmon, and the high frequency feature is ISP. Note that the absorption due to ISP occurs for $\omega > \Delta$, i.e., it is depolarization shifted. It is clear that ISP is well defined (represented by a sharp peak) only for small values of q . For sufficiently large values of q , it is Landau damped (it decays into the single particle excitations), which can be seen in Fig. 3 as a rapid broadening of the ISP peak with increasing q . The depolarization shift measures the fraction of the absorbed energy transferred to the collective motion of electrons associated with ISP. The remaining portion of the absorbed energy is used to transfer a single electron between the two subbands. When the population is inverted in this system, the absorption spectrum for small q is dominated by the negative (emissive) ISP peak, and the corresponding depolarization shift is also negative. The depolarization shift in this case measures the fraction of the energy transferred to the collective oscillations by an electron scattered from the upper to the lower subband. Thus, collective oscillations associated with ISP are generated whenever electrons are transferred between subbands. The most efficient buildup of these collective excitations can occur if both, downwards and upwards, electron transitions occur simultaneously. This can happen in a three-subband scenario [14], with a large population on the middle (2) subband, and almost empty bottom (1) and top (3) subbands. In this situation, the spectral response for small q consists of two peaks, one due to the ISP of the upper pair (3-2), upwards depolarization shifted, and one due to the ISP of the lower pair (2-1), downwards depolarization shifted from the corresponding intersubband separation. For some $\Delta_{21} > \Delta_{32}$, the two intersubband peaks can merge [14]. This is an attractive crossing, reflecting the resonant (stimulated) emission of two ISP. This can provide an efficient mechanism for off-resonant current enhancement in RTD. The rate of plasmon excitation is equal to the rate of the corresponding electron-electron transfer. Using the current balance analysis, it is easy to show that one can simulate the necessary conditions for this ISP resonant process (i.e., first and third subbands empty, and the second occupied), by employing an asymmetric RTD, with sufficiently thick barriers, and with the injector side barrier thicker than the collector one. This is consistent with the basic design of our structures, and therefore we can expect this phenomenon to occur in our RTD's. In fact, the observed off-resonant current peak is fully consistent with this process. The bias sensitivity, which leads to the peak formation in the I - V characteristics, is a result of the stringent requirement for a proper subband configuration, i.e., essentially $\Delta_{21} \approx \Delta_{32}$, needed for the resonant emission of ISP. This subband configuration, shown schematically in the inset of Fig. 1, can always be achieved in our RTD at a particular bias, not far from the middle point between the two current resonant peaks.

The above interpretation is fully confirmed by our detailed calculation for the structure C . To obtain the plasmon excitation rate, we follow the divergent solutions of the corresponding Dyson equation for the screened interaction in the complex frequency (ω) plane. We employ here the computational scheme published elsewhere [15]. Solutions with positive $\text{Im}(\omega)$ (in our convention) correspond to growing in time ISP, and the rate of this growth, $\gamma = \text{Im}(\omega)$. For our RTD structure C (or B) we find that there is an anticrossing of the two ISP at the expected bias corresponding to the $\Delta_{21} \approx \Delta_{32}$ condition. The resulting maximum scattering rate $\gamma_{\text{max}} = 1.02 \times 10^{-5}$ meV, is well above the estimated direct tunneling rate of about 10^{-9} meV at this bias. The corresponding current density is given by $j_{\text{max}} = en_{\text{pocket}}\gamma_{\text{max}} \approx 0.1$ A/cm⁻², where e is the electron charge, and n_{pocket} is the electron density in the pocket (on subband 2), and represents the maximum value of the Lorentzian broadened peak, shown as a thin solid line in Fig. 1. This calculated peak is in good quantitative agreement with experiment. We have used here a phenomenological broadening, which in our samples is most likely due to the interface roughness. In fact, one monolayer fluctuation on each interface of our RTD can easily account for the observed $\sim 10\%$ broadening.

We have also studied effects of the magnetic field applied along the growth direction of the structure C , and found that there is only a small, overall upwards shift of the entire I - V curve with increasing magnetic field. This suggests that the mechanism responsible for the peak involves primarily vertical (small q) electron transitions, supporting our interpretation. Applying a magnetic field to sample B leads to formation (in the off-resonant tunneling domain) of Landau level peaks expected in the system which, in the absence of a magnetic field, is dominated by elastic (large q) scattering. This is in full agreement with our interpretation above. Finally, we have excluded the impurity states inside the RTD as the source of the peak. The I - V curves of Fig. 1 show that the quality of sample C is even higher than that of samples B and A .

In conclusion, we have reported here the first observation of the off-resonant tunneling mediated by the resonant emission of the intersubband plasmons, in a RTD structure with a very long emitter drift region. This process involves the resonant plasmon mode interaction, and can occur in samples with a minimum of three subbands, and with a population inversion between two of the three. In addition, the sample must have sufficiently low defect density so as to allow for electron transitions with very small in-plane momenta, necessary to avoid the Landau damping. The very long drift region stimulates formation of the potential pocket at the RTD on the emitter side. Tunneling from the pocket is enhanced, and this effectively "inserts" the filled emitter subband between the two empty subbands of the RTD, creating the desired three subband scenario. Our detailed calculations are in quantitative agreement with the experiment, and confirm fully our interpretation of

the strong off-resonant peak in the I - V characteristic of our structure.

We thank Kevin Bedell and Jan Engelbrecht for useful discussions. This work was supported in part by the U.S. Army Research Office No. DAAD 19-99-1-0121.

-
- [1] B. Ricco and M. Ya. Azbel, Phys. Rev. B **29**, 1970 (1984).
[2] R. Tsu and L. Esaki, Appl. Phys. Lett. **22**, 562 (1973).
[3] E.R. Brown, W.D. Goodhue, and T.C.L.G. Sollner, J. Appl. Phys. **64**, 1519 (1988); F. Beltram and F. Capasso, in *The Physics of Low-Dimensional Semiconductor Structures*, edited by Butcher *et al.* (Plenum, New York, 1993); J. Faist, F. Capasso, C. Sirtori, D.L. Sivco, and A.L. Hutchinson, Phys. Rev. Lett. **76**, 411 (1996).
[4] V.J. Goldman, D.C. Tsui, and J.E. Cunningham, Phys. Rev. B **36**, 7635 (1987); G.S. Boebinger, A.F.J. Levi, S. Schmitt, A. Passner, L.N. Pfeiffer, and K.W. West, Phys. Rev. Lett. **65**, 235 (1990); Das Sarma, Phys. Rev. Lett. **52**, 859 (1984).
[5] H. Drexler, J.S. Scott, S.J. Allen, K.L. Campman, and A.C. Gossard, Appl. Phys. Lett. **67**, 2816 (1995).
[6] C. Zhang, M.L.F. Lerch, A.D. Martin, P.E. Simmonds, and L. Eaves, Phys. Rev. Lett. **72**, 3397 (1994).
[7] T.K. Ng and P.A. Lee, Phys. Rev. Lett. **61**, 1768 (1988).
[8] J. Leo and A.H. MacDonald, Phys. Rev. Lett. **64**, 817 (1990).
[9] We used the Thomas-Fermi-Poisson code of G. Snider, available free of charge at www.nd.edu/~gsnider/. We showed before, by comparing it with our own results, that this code is a reliable, fast, and user friendly tool to estimate a ground state (or even a nonequilibrium steady state) of various quantum well systems.
[10] See, for example, A.P. French and E.F. Taylor, *Introduction to Quantum Physics*, M.I.T. Introductory Physics Series (Norton, New York, 1978).
[11] P. Hylgaard and J. Wilkins, Phys. Rev. B **53**, 6889 (1996).
[12] K. Kempa, P. Bakshi, J. Engelbrecht, and Y. Zhou, Phys. Rev. B **61**, 11 083 (2000).
[13] S.C. Lee and I. Galbraith, Phys. Rev. B **55**, R16025 (1997).
[14] P. Bakshi and K. Kempa, *Condensed Matter Theories*, edited by J.W. Clark and P.V. Panat (Nova Science Publishers, New York, 1997), Vol. 12, pp. 399–412.
[15] K. Kempa, D.A. Broido, C. Beckwith, and J. Cen, Phys. Rev. B **40**, 8385 (1989).